Microscale instability and mixing in driven and active suspensions

Michael Shelley, Applied Math Lab, Courant Institute

Collaborators:

Lisa Fauci	Tulane
Christel Hohenegger	CIMS
Eric Keaveny	CIMS
David Saintillan	UIUC
Joseph Teran	UCLA
Becca Thomases	UC-Davis

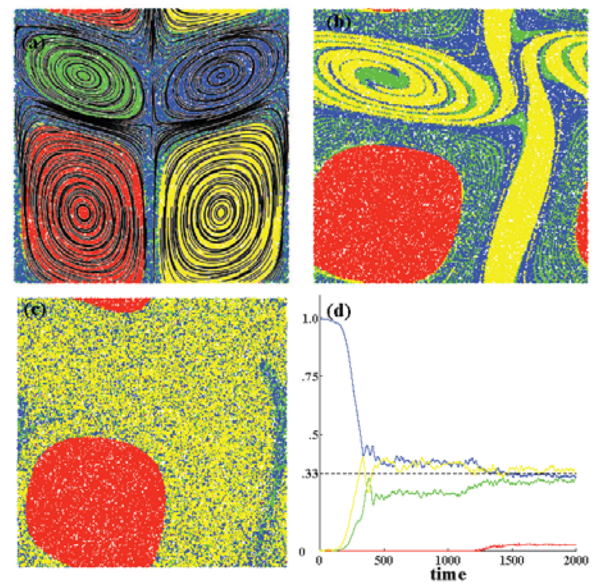

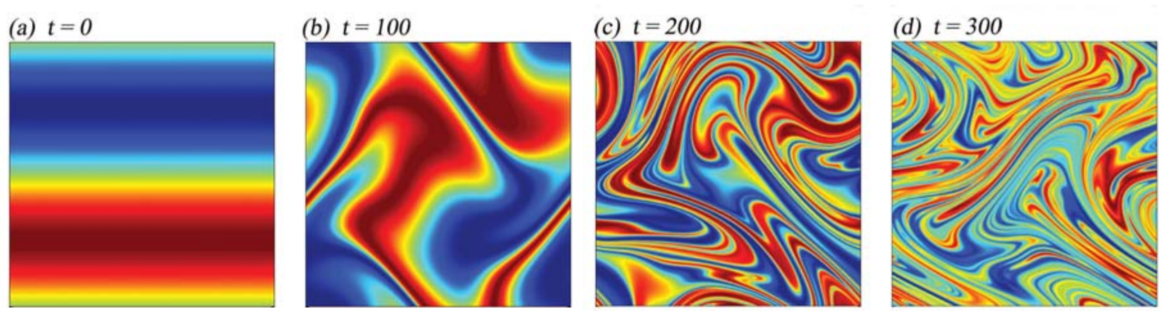

Dynamics and interactions of micro-structure in complex fluids

- Dynamics of non-Newtonian fluids
- Reinforced composite materials
- Biological locomotion
- Elastic “turbulence” & low *Re* mixing

  Groisman & Sternberg ’00, ’01, …
- Microfluidic rectifiers

  Groisman, Enzelberger, & Quake ‘03

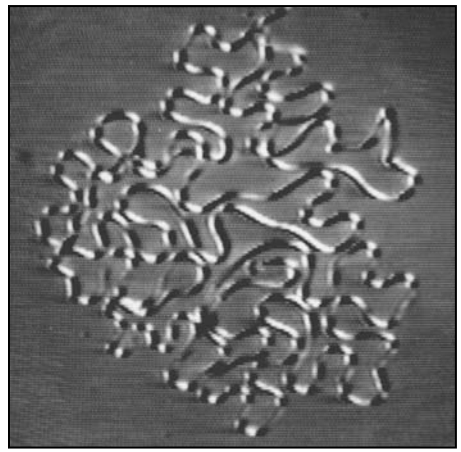

I-S_A phase trans -- PPM

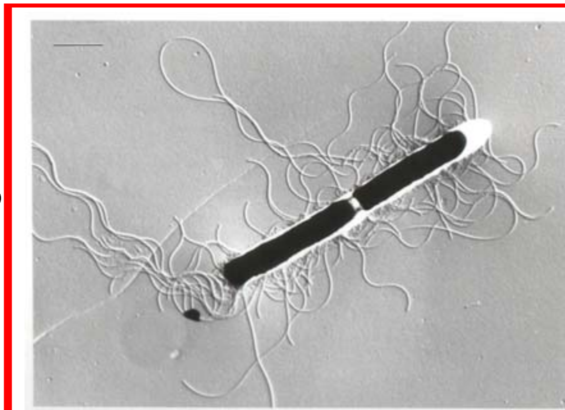

B. subtilis – one and many

C. Dombrowski et al ’05, 07

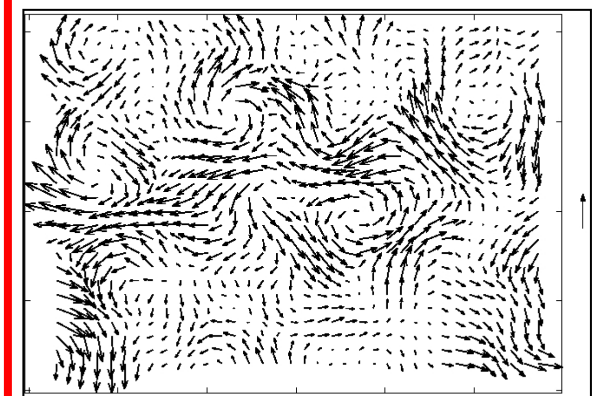

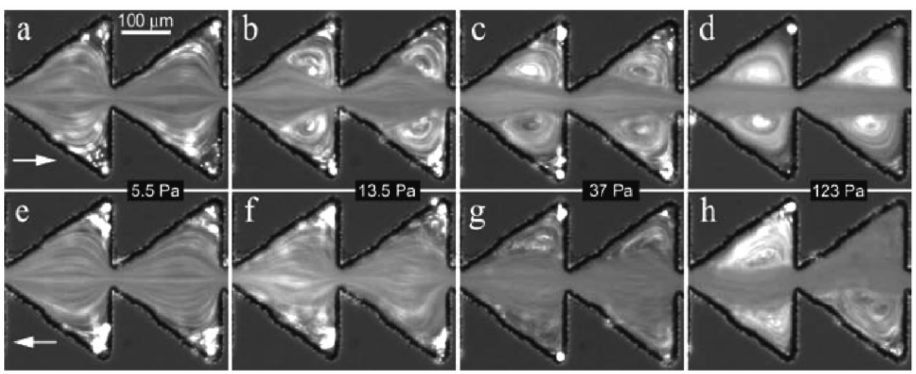

microfluidic rectifier – Groisman & Quake

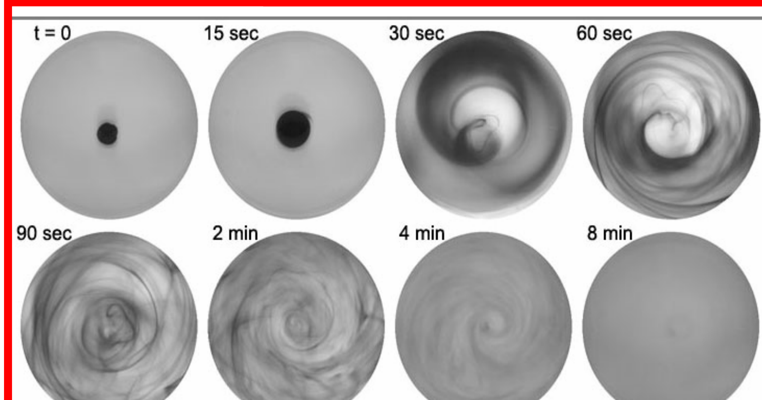

microscale mixing – Groisman & Steinberg

Experiments: V. Steinberg & A. Groisman

Viscoelastic fluid – Elastic "turbulence" - Efficient mixing

Rotating plates (Low Re, "High" Wi)

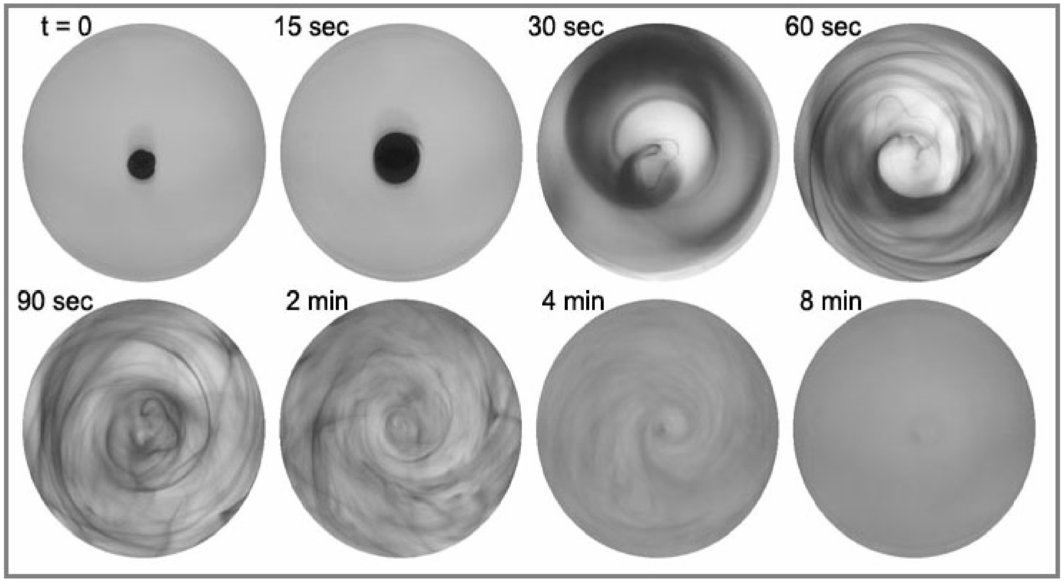

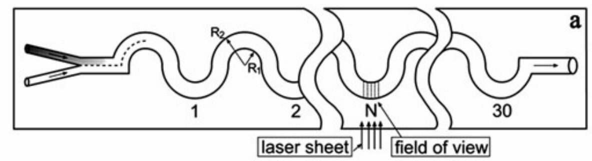

Mixing in micro channels

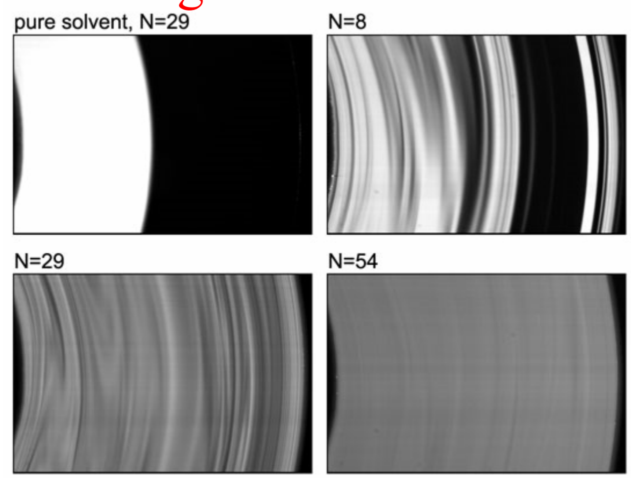

Arratia *et al*, *PRL 2006*

Elastic fluid instabilities near hyperbolic points

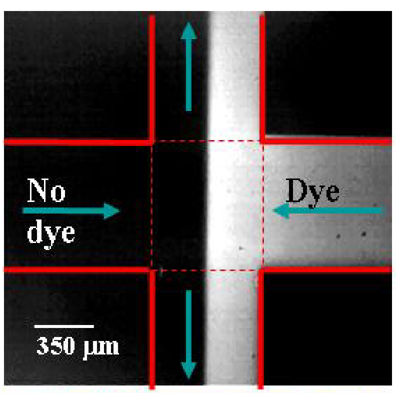

(b)

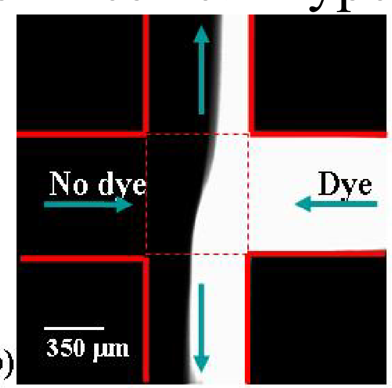

(c)

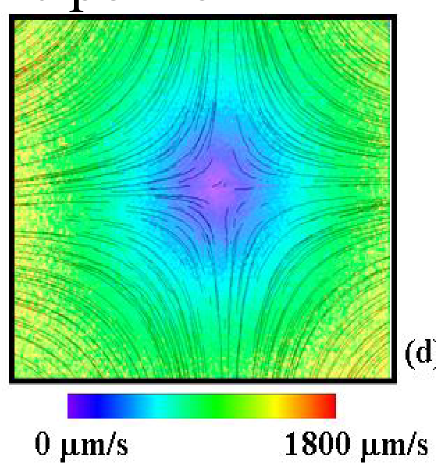

(d)

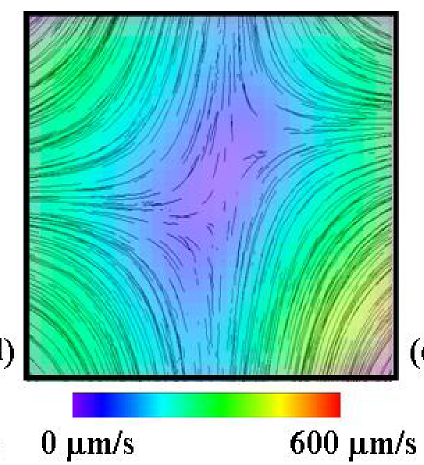

(e)

Stokes-Oldroyd-B (*Re<<1*)

- model of a “Boger” elastic fluid (normal stresses, no shear thinning)
- derives from a microscopic, dilute theory of polymer coils
- one of the standard viscoelastic flow models; Little known about large data solutions.

$$-\nabla p + \Delta \mathbf{u} = -\beta \nabla \cdot \boldsymbol{\sigma}_\mathbf{p} - \mathbf{f} \quad \text{and} \quad \nabla \cdot \mathbf{u} = 0$$

momentum and mass balance

$$Wi\ \boldsymbol{\sigma}_\mathbf{p}^{\nabla} = -(\boldsymbol{\sigma}_\mathbf{p} - \mathbf{I})$$

transport and dissipation of polymer stress

- $\boldsymbol{\sigma}_\mathbf{p}^{\nabla} = \frac{D\boldsymbol{\sigma}_\mathbf{p}}{Dt} - (\nabla \mathbf{u} \cdot \boldsymbol{\sigma}_\mathbf{p} + \boldsymbol{\sigma}_\mathbf{p} \cdot \nabla \mathbf{u}^\mathrm{T})$ Upper convected time derivative

$$\tau_f = \frac{\mu}{\rho L F}$$

- $Wi = \frac{\tau_p}{\tau_f}$; Weissenberg number — ratio of polymer relax. time to flow time-scale
- $\beta = \frac{G\tau_f}{\mu}$; coupling strength

μ = solvent viscosity; F = external force scale
τ_p = polymer relaxation time; G = background poly. stress

- $\beta \cdot Wi = \frac{G\tau_p}{\mu} = \frac{\text{polymer viscosity}}{\text{solvent viscosity}}$ — Material constant; fix to ½ as in expts of Arratia *et al*

Properties:

(1) Has decaying "strain" energy: $E = \frac{1}{2}\int \mathrm{tr}\left(\boldsymbol{\sigma}_\mathbf{p} - \mathbf{I}\right)$

$$\dot{E} + Wi^{-1}E = 2\beta^{-1}\left[-\int |\nabla \mathbf{u}|^2 + \int \mathbf{u}\cdot\mathbf{f}\right]$$

(2) But lacks of scale dependent dissipation:

$$\frac{\partial \hat{\boldsymbol{\sigma}}_p}{\partial t} = L(\hat{\mathbf{k}})\hat{\boldsymbol{\sigma}}_p + P(\hat{\mathbf{k}})\hat{\mathbf{f}}$$

with $\hat{\mathbf{k}} = \mathbf{k}/|\mathbf{k}|$

Use the Fourier transform to solve the linearized problem

(3) Polymer stress tensor: $\boldsymbol{\sigma}_\mathbf{p} = \nu\langle \mathbf{fr}\rangle = C\langle \mathbf{rr}\rangle$ ← Assume linear Hooke's law for bead forces

is s.p.d.

(4) Existence of large-data solutions is unknown, even in 2d

Simulations: De-aliased Fourier based spectral method; second order time stepping.

Vorticity field for Newtonian fluid

Four – roll mill geometry

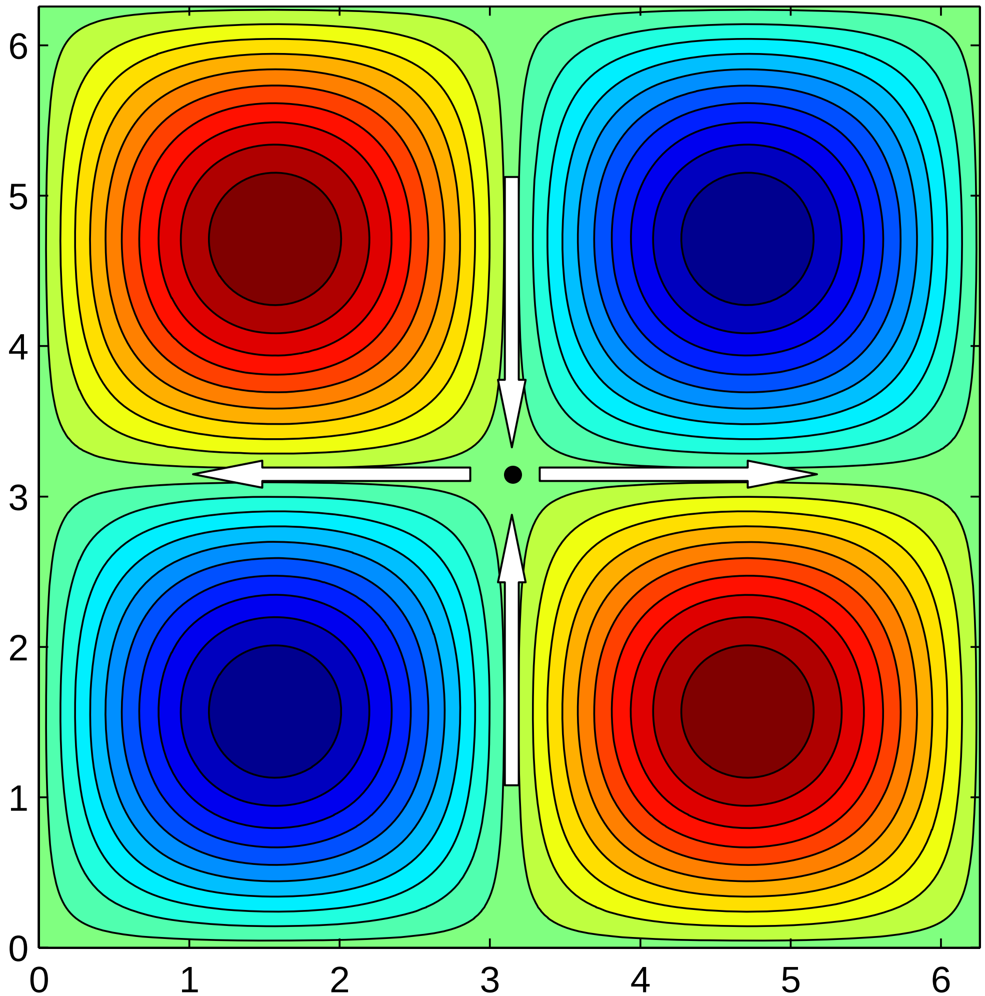

Thomases & Shelley *PF* 2007

Background force

$$\mathbf{f} = \begin{pmatrix} -2\sin x \cos y \\ 2\cos x \sin y \end{pmatrix}$$

With Newtonian fluid yields

$$\mathbf{u} = \begin{pmatrix} \sin x \cos y \\ -\cos x \sin y \end{pmatrix}$$

Creates hyperbolic points in background flow
ala Arratia *et al.*, *PRL* 2006

Also Berti et al '08, Xi & Graham '09
Becherer, Morozov, van Saarloos '08, 09

Evolution for initial stress: $\boldsymbol{\sigma}_p(t=0)=\mathbf{I}$

$\omega \rightarrow$

$\mathrm{tr}(\boldsymbol{\sigma}_p) \rightarrow$

slices of $\boldsymbol{\sigma}_p^{11} \rightarrow$

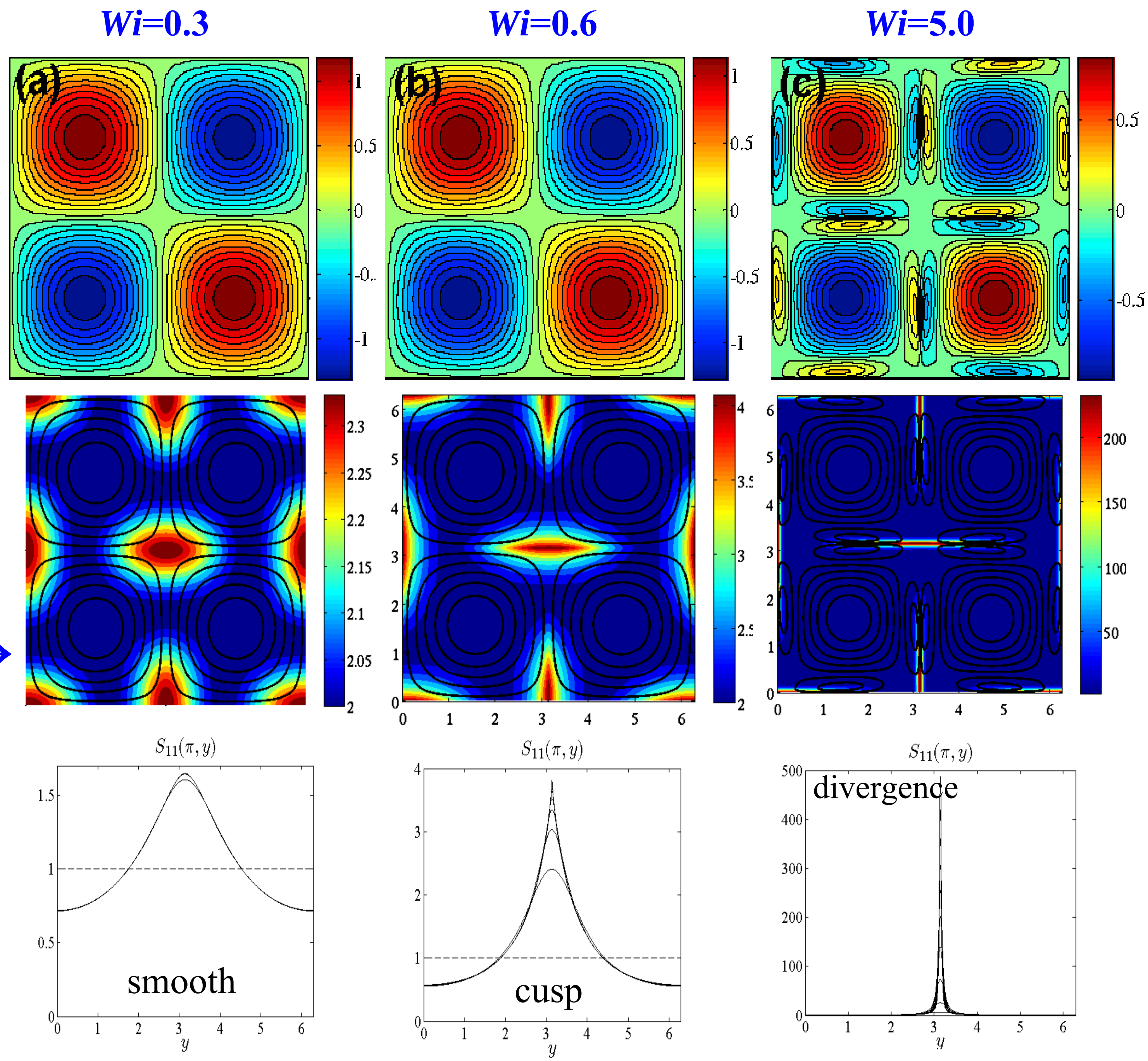

Local Model – fix strain-rate α – determined by flow -- and advect stress field by local straining velocity

$$\tilde{u} = (\alpha x, -\alpha y); \quad \varphi = \sigma_p^{11}; \quad t \to Wi \cdot t \; ; \; \varepsilon = \alpha \cdot Wi$$

$$\boxed{\varphi_t + \varepsilon x \varphi_x - \varepsilon y \varphi_y + (1-2\varepsilon)\varphi - 1 = 0}$$

General solution :

$$\boxed{\varphi = \frac{1}{1\text{-}2\varepsilon} + e^{(2\varepsilon-1)t} H_{11}(xe^{-\varepsilon t}, ye^{\varepsilon t})}$$

Relevant solution : $H_{11}(a,b) = h(b)$ with $h(b) \sim |b|^q$ as $|b| \to \infty$

Why? Choose q to eliminate long time t – dependence

$$\Rightarrow q = \frac{1-2\varepsilon}{\varepsilon} \Rightarrow \boxed{\varphi|_{t\to\infty} = \frac{1}{1-2\varepsilon} + C\,|\,y\,|^{\frac{1-2\varepsilon}{\varepsilon}}}$$

steady states also studied by Rallison & Hinch '88 and M. Renardy '06

$$\varepsilon = \alpha(Wi)\,Wi; \quad q = \frac{1-2\varepsilon}{\varepsilon}$$

$$\varepsilon_1 = 1/3 \quad Wi_1 \approx 0.5$$

$$\varepsilon_2 = 1/2 \quad Wi_2 \approx 0.9$$

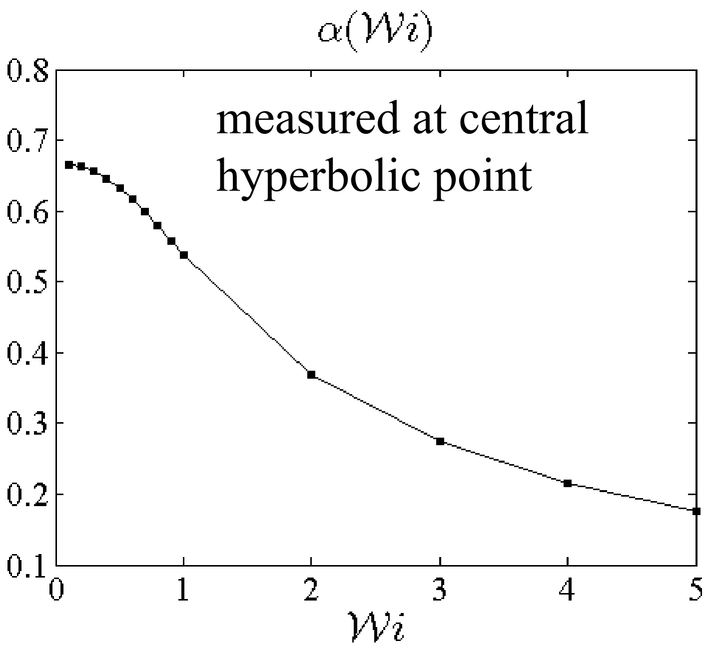

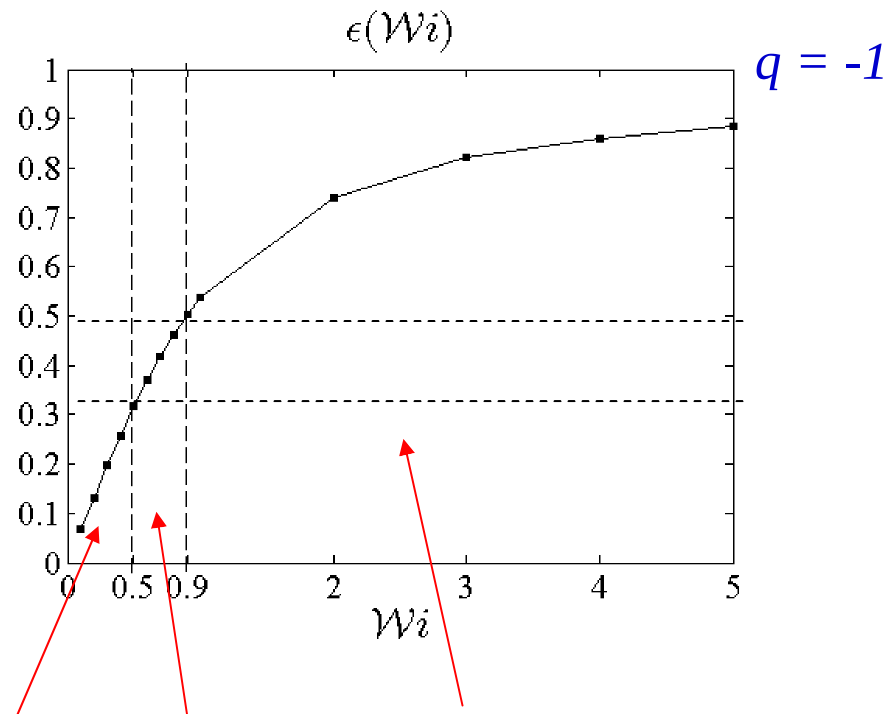

q > *1*

0 < *q* < *1*

cusp in stress

q < *0*

Divergence in stress

Note $\varepsilon < 1$ implies $q > -1$ so the stress is integrable.

<u>Mixing and Symmetry-Breaking:</u> Thomases & Shelley '09

The SOB system is also unstable to symmetry-breaking; see Poole *et al* '07, Xi & Graham '08

$\boldsymbol{\sigma}_p(0) - \mathbf{I} \sim O(10^{-2})$

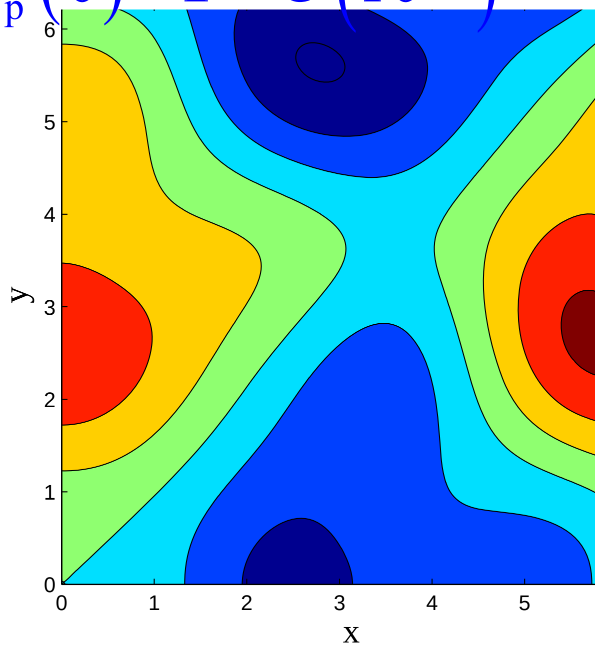

$\omega(0) - \omega_{Stokes}$

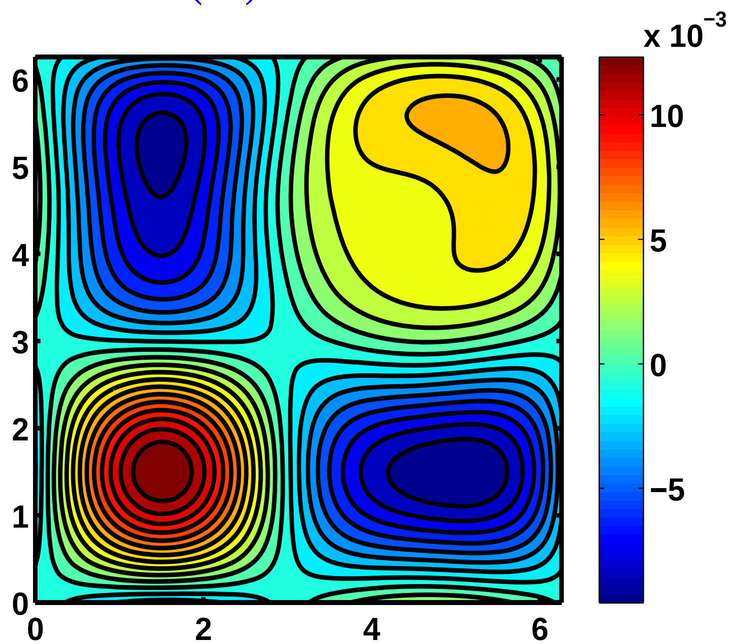

Full disclosure: Small amount of polymer stress diffusion added to control gradient growth

Long-time behavior with increasing *Wi*:

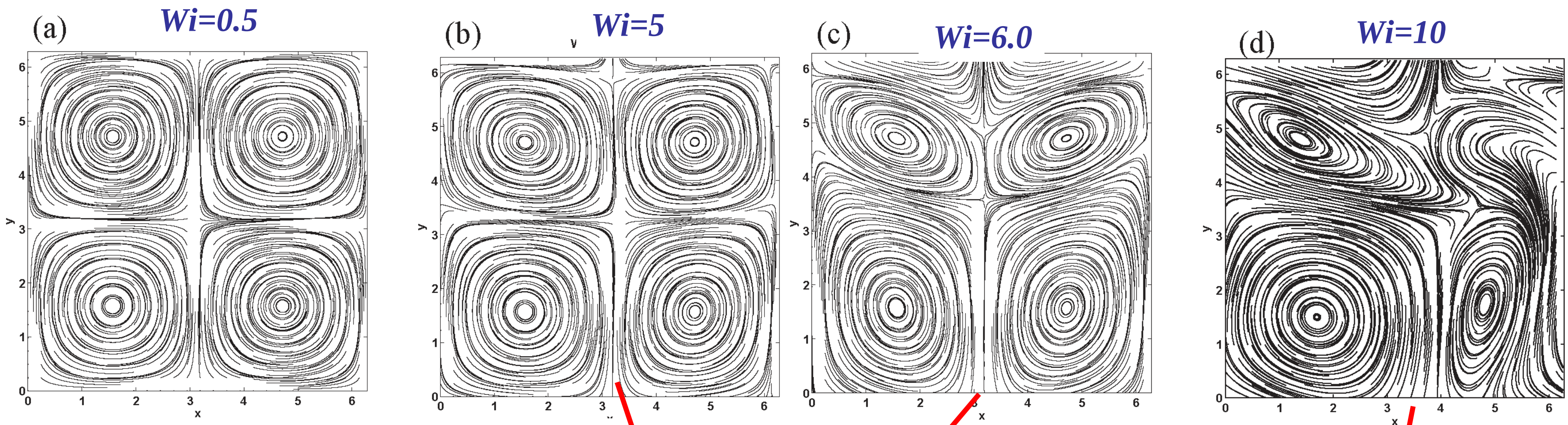

relaxation to
symmetric state

Slow relaxation
to asymmetric state

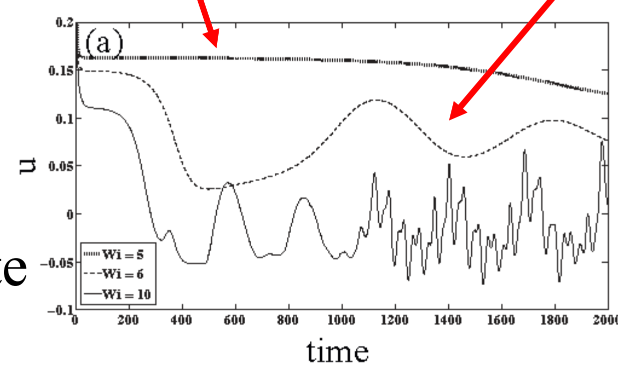

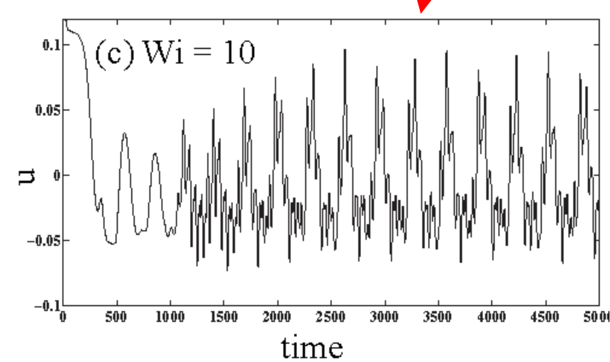

Persistent
oscillations

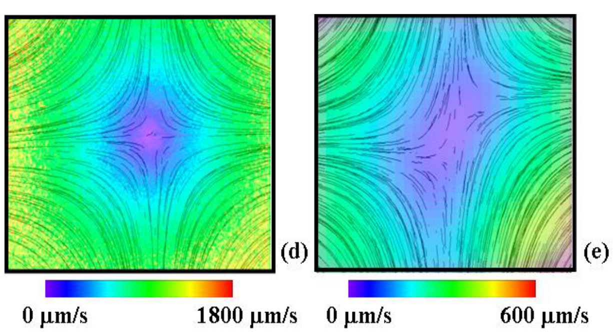

Arratia *et al '06*

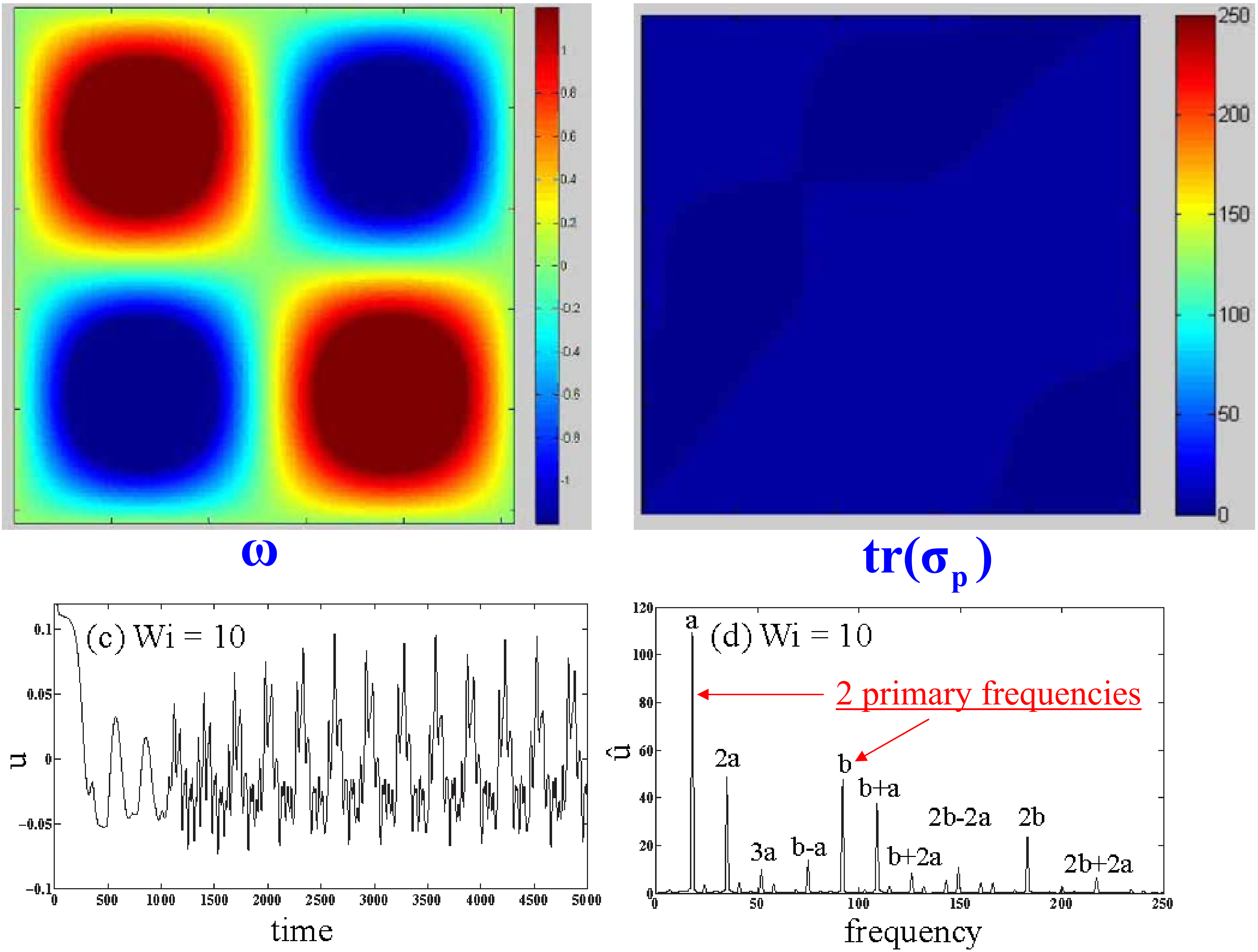
ω
tr(σp)
250
200
150
100
50
0
(c) Wi = 10
u
time
0.1
0.05
0
−0.05
−0.1
0 500 1000 1500 2000 2500 3000 3500 4000 4500 5000
(d) Wi = 10
û
frequency
120
100
80
60
40
20
0
0 50 100 150 200 250
2 primary frequencies
a
2a
3a
b-a
b
b+a
b+2a
2b-2a
2b
2b+2a

Wi=6, t=2000

Smaller *Wi:*
symmetry breaking, little mixing

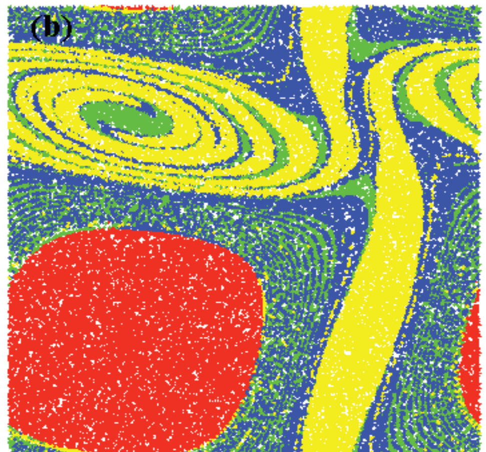

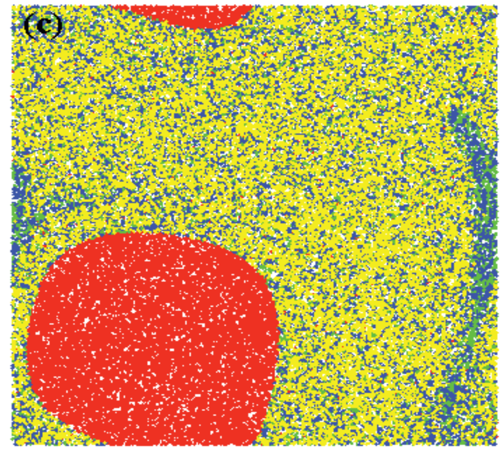

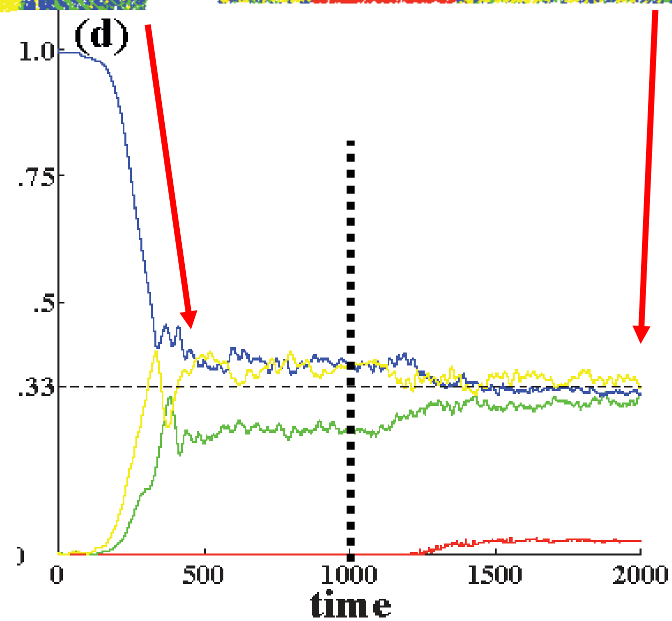

Larger *Wi*:

- multiple frequencies of oscillation
- robust GRS of viscoelastic flows
- well-mixed fluid outside of GRS

Need new experiments,
stability analyses.

Update:

(1) 1 of 10 simulations using random amplitude/phase initial perturbations for polymer stress.

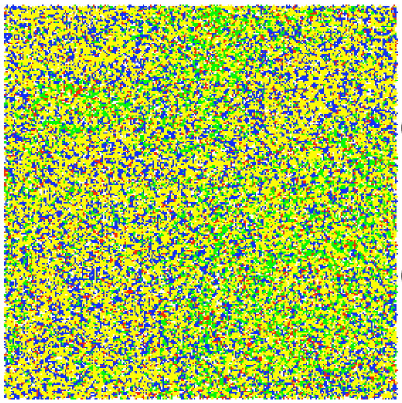

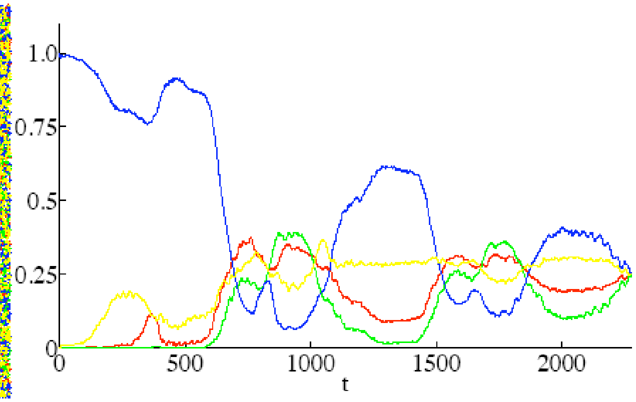

(2) What if the number of vortex cells is increased?

(3) Now investigating in a new expt'l rig in the AML

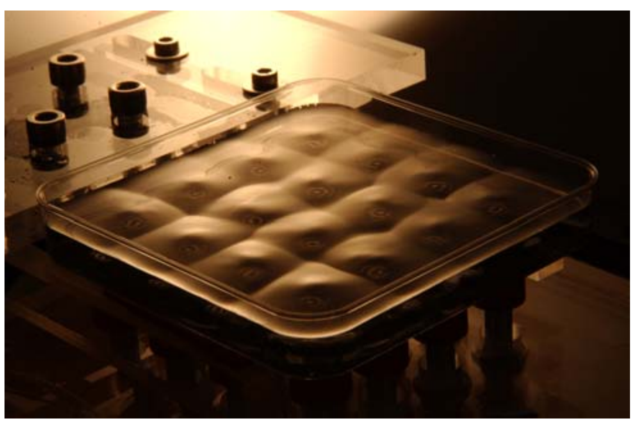

16 counter-rotating rotors driving a PAA viscoelastic solution

w. Bin Liu, J. Zhang

Collective dynamics of active suspensions (bacterial baths)

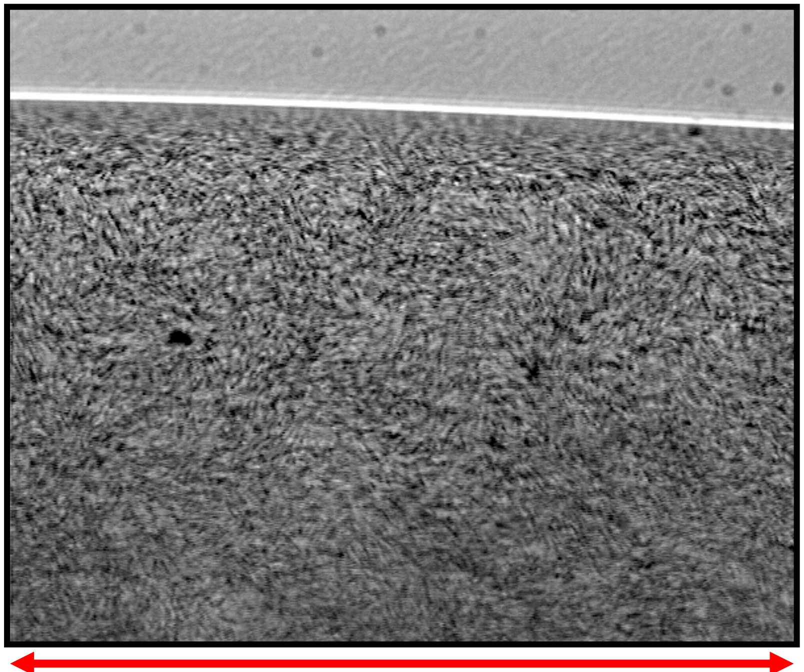

150 μm

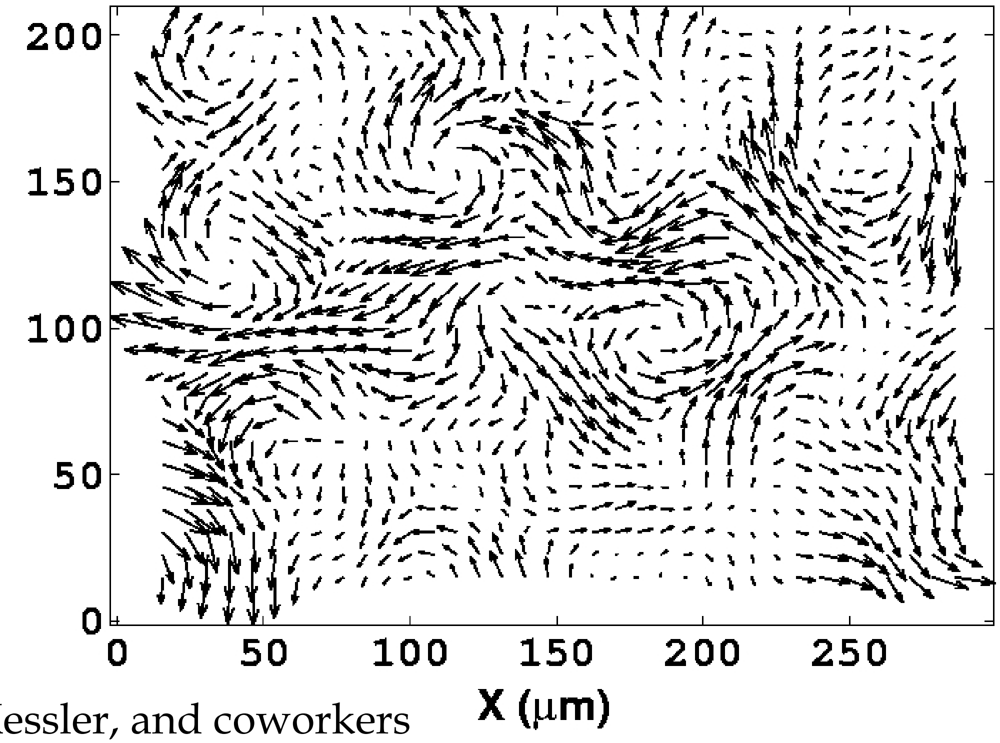

R. Goldstein, J. Kessler, and coworkers

Observation: meandering jet and vortices of scale 50-100 μm, speeds 50-100 μm/sec in jets
Scale of *B. subtilis* ~ 4 μm (plus tail); swimming speed 20-30 μm/sec

- A complex fluid driven by dynamics of its microstructure –
  many body interactions mediated by fluid.
- collective behavior leads to strong mixing.
- Role of body geometry? Emergence or role of orientational ordering?
- Competition of hydrodynamic coupling vs. attractive gradients?

Some of the experiments:

- Wu & Libchaber '00:"brownian" motion of test particles in bacterial baths.
- Dombrowski *et al* '04: large-scale flow structures (many body lengths).
- Kim & Breuer '04, enhanced mixing using bacteria in micro-fluidic device.
- Paxton *et al*, '04, fabricated chemically-driven nano-rod-swimmers.
- Dreyfus *et al*, '05, bio-mimetic swimmers driven by magnetic fields
- Short *et al*, 06, expts and model of *Volvox* swimming.
- Sokolov *et al*, '07, expts on concentration dependencies in thin films.
- …

Some of the theory:

- bioconvection: Childress & Spiegel, Pedley and many others
- Simha & Ramaswamy '02: predict instability of long-wave oriented states
- Hernandez-Ortiz *et al*, '05: simulations of force-dipole suspensions show emergence of large-scale structures
- Toner *et al*, '05: models of flocking.
- Sambelashvili, Lau, & Cai '07, ordering of 2d rod locomotors by local steric interactions
- Pedley, Ishikawa *et al*, interactions of *squirmers* (specified surface velocity)
- Saintillan & Shelley, 07, '08, particle simulations, kinetic theory of moving rod suspensions
- Keaveny & Maxey, '08, theory and simulations for bio-mimetic swimmers
- Kanevsky et al, '09, simulations of interacting stress-actuated swimmers
- …

Slender-body swimmer driven by surface stress

Saintillan & Shelley *PRL* 2007 , motivated by Volvox model of Short, Goldstein, *et al*;
(simulation of multi-V interactions by Kanevsky, Shelley, Tornberg, '08)

Surface tractions:

$$\boldsymbol{\sigma}(s,\theta)\cdot\boldsymbol{n} = \underbrace{f_0(s)\boldsymbol{t}}_{\text{prescribed}} + \underbrace{g(s,\theta)\boldsymbol{n}}_{\text{unknown}}$$

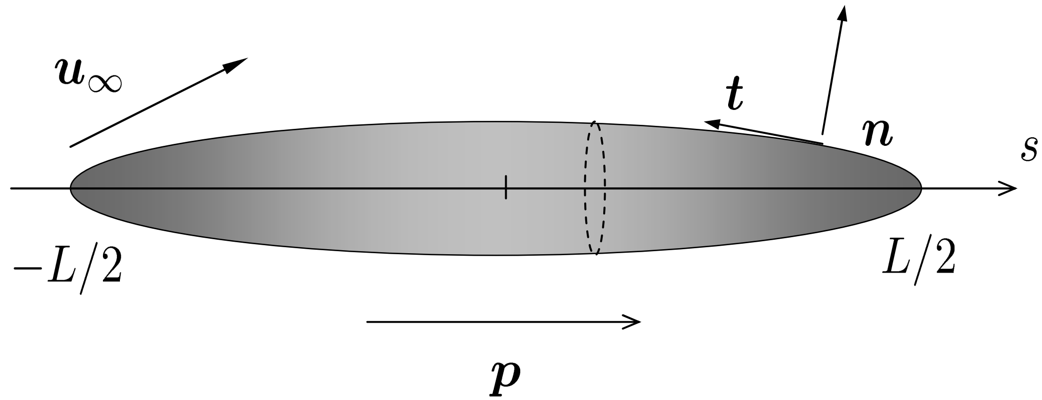

Integrated traction (force per unit length):

$$\boldsymbol{f}(s) = \int_0^{2\pi} \boldsymbol{\sigma}(s,\theta)\cdot\boldsymbol{n}\, r(s)\mathrm{d}\theta = \underbrace{2\pi f_0(s)r(s)m(s)\boldsymbol{p}}_{\substack{\boldsymbol{f}_\parallel,\ \text{prescribed} \\ (\, m(s)=\boldsymbol{t}(s)\cdot\boldsymbol{p}\,)}} + \underbrace{\boldsymbol{f}_\perp(s)}_{\text{unknown}}$$

Force and torque balances:

$$\boldsymbol{F} = \int_{-L/2}^{L/2} \boldsymbol{f}(s)\mathrm{d}s = \mathbf{0}, \quad \boldsymbol{T} = \int_{-L/2}^{L/2} s\boldsymbol{p}\times\boldsymbol{f}(s)\mathrm{d}s = \mathbf{0}$$

Single particle flow fields

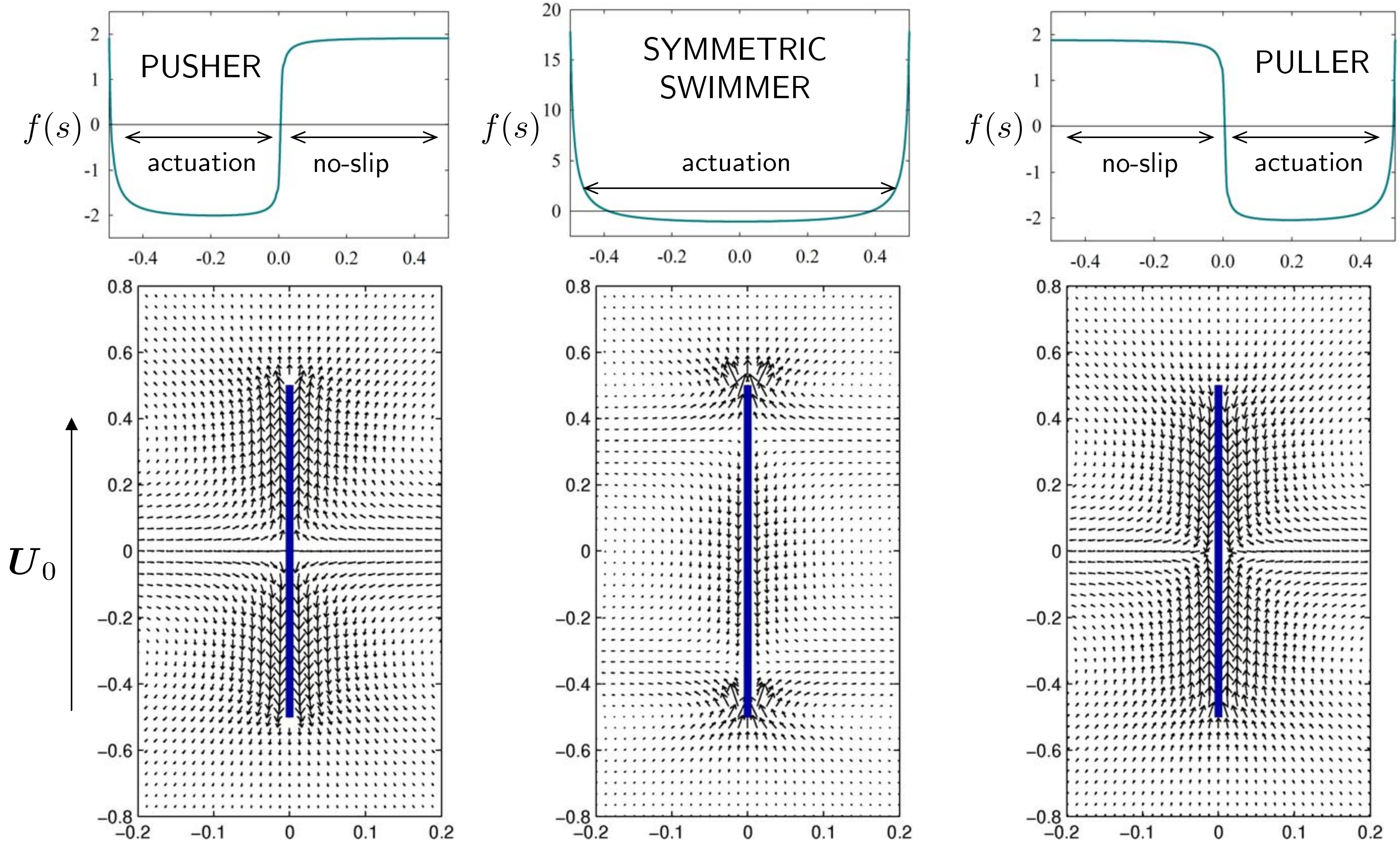

FAR FIELD:

$$|\boldsymbol{u}(\boldsymbol{x})| \sim U_0 \left(\frac{L}{|\boldsymbol{x}|} \right)^2$$
(stresslet)

$$|\boldsymbol{u}(\boldsymbol{x})| \sim U_0 \left(\frac{L}{|\boldsymbol{x}|} \right)^3$$
(Stokes quadrupole)

$$|\boldsymbol{u}(\boldsymbol{x})| \sim U_0 \left(\frac{L}{|\boldsymbol{x}|} \right)^2$$
(stresslet)

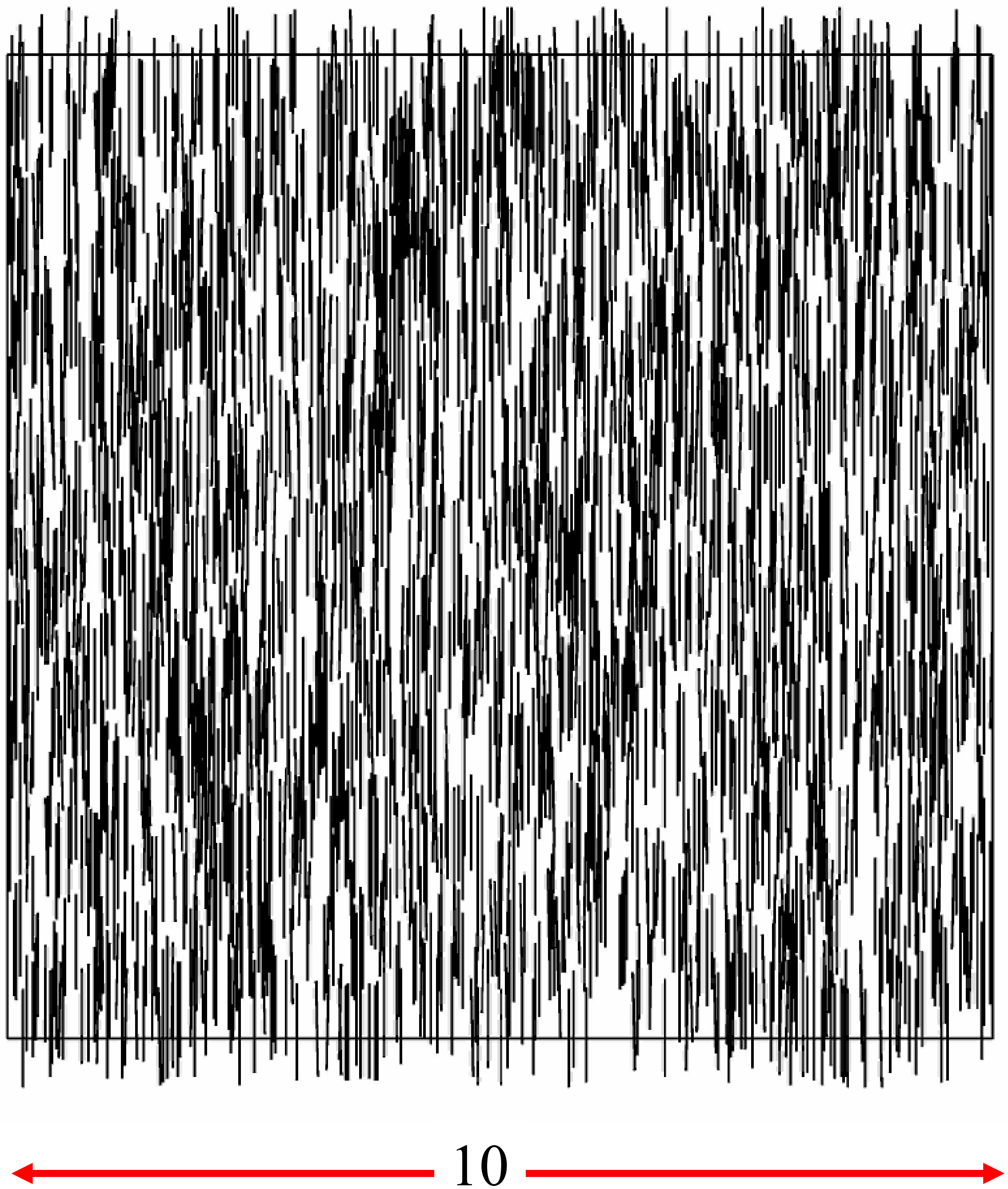

Saintillan & Shelley, *PRL '07*

2500 swimming "pushers" in periodic box of dimensions

10 x 10 x 3

effective volume fraction $n\,(L/2)^3 = 1$; n = # density (strongly interacting)

All initially aligned in the **z** direction – nematic order – with randomized positions

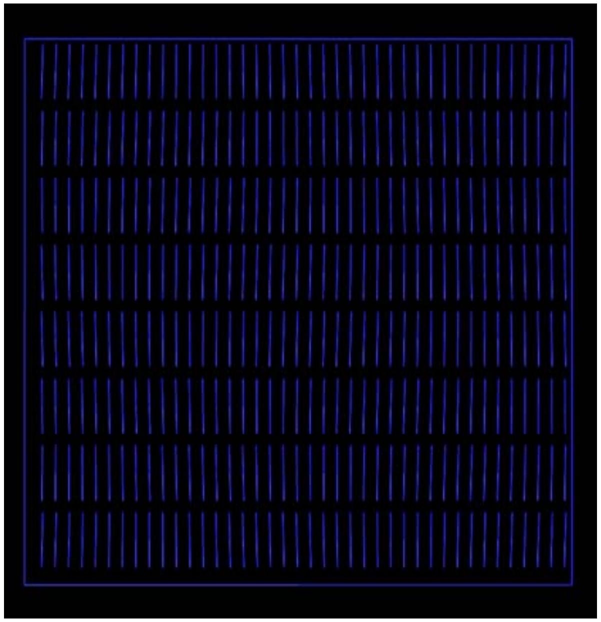

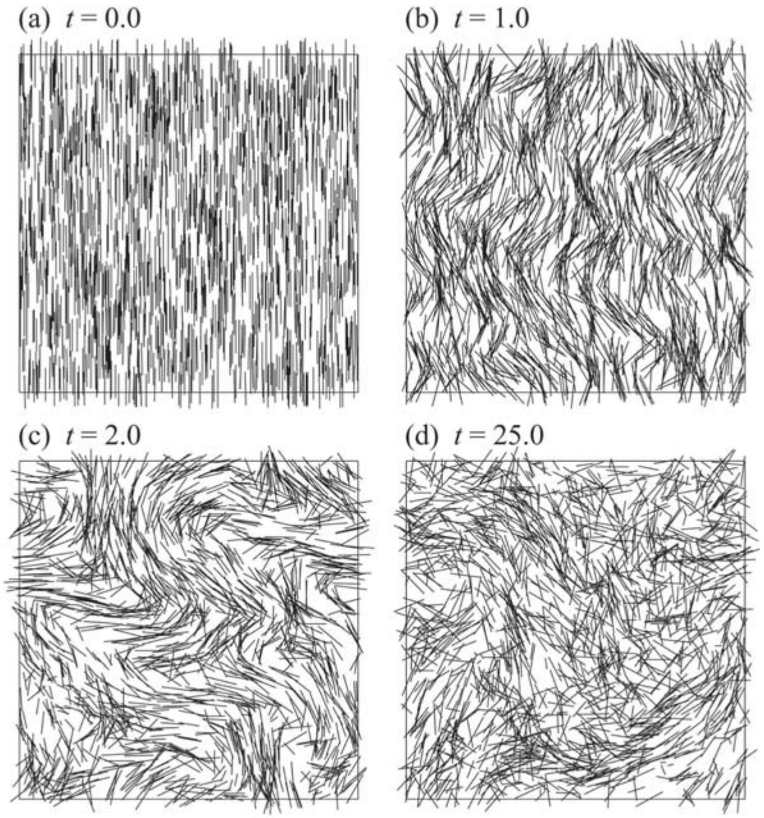

Spatially organized instability destroys long-range order. Predicted by Simha & Ramaswamy ‘02

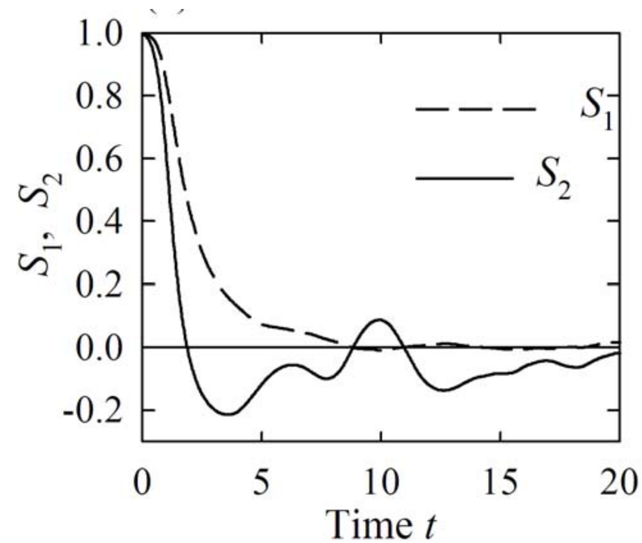

Loss of global orientational order:

order parameters:

$$S_1 = \langle \mathbf{p} \cdot \mathbf{z} \rangle \quad \& \quad S_2 = \frac{1}{2}\left(3\langle \mathbf{p} \cdot \mathbf{z} \rangle^2 - 1\right)$$

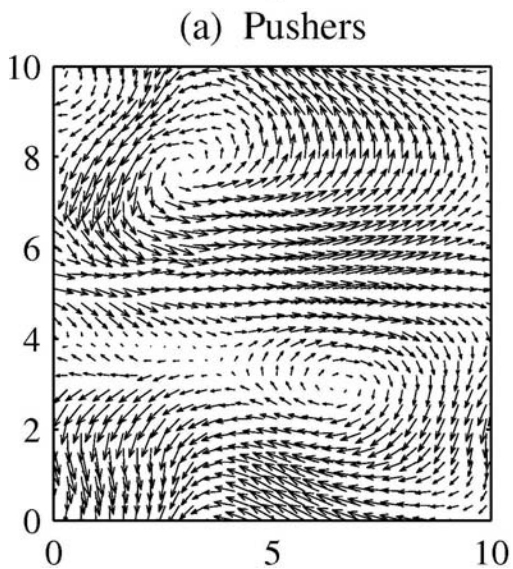

Emergence of large-scale dynamical flow as in Dombrowski *et al*, Hernandez-Ortiz *et al*

A kinetic theory for active suspensions S&S, *PRL* '08, *PF* '08

Pose Fokker-Planck equation for distribution function $\Psi(\mathbf{x},\mathbf{p},t)$ of particle center of mass $\mathbf{x}$ and (unit) swimming director $\mathbf{p}$ (rod theory, Doi & Edwards, '86) :

$$\Psi_t + \nabla_x \cdot (\dot{\mathbf{x}}\Psi) + \nabla_p \cdot (\dot{\mathbf{p}}\Psi) = 0 \quad \text{with} \quad \frac{1}{V}\int dV_x \int dS_p \Psi = n$$

w. "particle" fluxes
$$\begin{cases} \dot{\mathbf{x}} = U_0\,\mathbf{p} + \mathbf{u}(\mathbf{x},t) - \nabla_x (D \ln \Psi) \\ \dot{\mathbf{p}} = (\mathbf{I} - \mathbf{pp})(\gamma \mathbf{E} + \mathbf{W})\mathbf{p} - \nabla_p (d \ln \Psi) \end{cases}$$

Background fluid velocity:

$$\nabla q - \Delta \mathbf{u} = \nabla \cdot \boldsymbol{\Sigma}^a \quad \text{and} \quad \nabla \cdot \mathbf{u} = 0$$

driven by active swimming stress (Kirkwood theory; Batchelor '70):

$$\boldsymbol{\Sigma}^a(\mathbf{x},t) = \sigma_0 \int dS_p \Psi(\mathbf{x},\mathbf{p},t)[\mathbf{pp} - \mathbf{I}/3]$$

Pushers: $\sigma_0 < 0$; *Pullers*: $\sigma_0 > 0$

Important d'less parameters: $U_0 \to 1,\ \sigma_0 \to \alpha = O(1),\ L \to L/l_c$

A useful special case

Neglecting diffusion, consider a locally aligned suspension:

$$\Psi(\mathbf{x},\mathbf{p},t) = c(\mathbf{x},t)\,\delta\left(\mathbf{p}-\mathbf{n}(\mathbf{x},t)\right)$$

Setting *D=d=0* The full kinetic equations reduce exactly to:

$$\begin{cases} \dfrac{\partial c}{\partial t} + \nabla_x \bullet \left((\mathbf{n}+\mathbf{u})\, c \right) = 0 \\ \dfrac{\partial \mathbf{n}}{\partial t} + (\mathbf{n}+\mathbf{u}) \bullet \nabla_x \mathbf{n} = (\mathbf{I} - \mathbf{nn}) \nabla_x \mathbf{u}\, \mathbf{n} \end{cases}$$

(preserves $\mathbf{n} \bullet \mathbf{n} = 1$)

with $\nabla_x q - \nabla_x^2 \mathbf{u} = -\nabla_x \bullet \boldsymbol{\Sigma}^a, \qquad \nabla_x \bullet \mathbf{u} = 0$

and particle extra stress $\boldsymbol{\Sigma}^p = \alpha\, c(\mathbf{x},t)\left(\mathbf{nn} - \mathbf{I}/3\right)$

Stability analysis II: uniform isotropic case

A nearly isotropic uniform suspension:

$$\Psi(\mathbf{x},\mathbf{p},t)=\frac{1}{4\pi}\left[1+\varepsilon\tilde{\Psi}_{\mathbf{k}}(\mathbf{p})e^{i(\mathbf{k}\cdot\mathbf{x}+\lambda t)}\right]$$

Derive relation:

$$\boxed{\tilde{\Psi}_{\mathbf{k}}=-\frac{3i\alpha\gamma}{2\pi}\frac{\hat{\mathbf{k}}\cdot\mathbf{p}}{\lambda+i\mathbf{k}\cdot\mathbf{p}+Dk^2}\,\mathbf{p}\cdot\mathbf{F}\left[\tilde{\Psi}_{\mathbf{k}}\right]} \qquad (1)$$

where

$$\mathbf{F}\left[\tilde{\Psi}_{\mathbf{k}}\right]=\left(\mathbf{I}-\hat{\mathbf{k}}\hat{\mathbf{k}}\right)\int dS_{p'}\,\mathbf{p}'\left(\hat{\mathbf{k}}\cdot\mathbf{p}'\right)\tilde{\Psi}_{\mathbf{k}}(\mathbf{p}')$$

Applying **F** operator to (1), and evaluation of the integral,

yields the eigenvalue relation:

$$\frac{3i\alpha\gamma}{2k}\left[2a^3-\frac{4}{3}a+\left(a^4-a^2\right)\log\frac{a-1}{a+1}\right]=1 \quad \text{w.} \quad a=-i\left(\lambda+Dk^2\right)/k$$

$\alpha = -1$ (pushers), $\gamma = 1$ (rods), $D = 0$

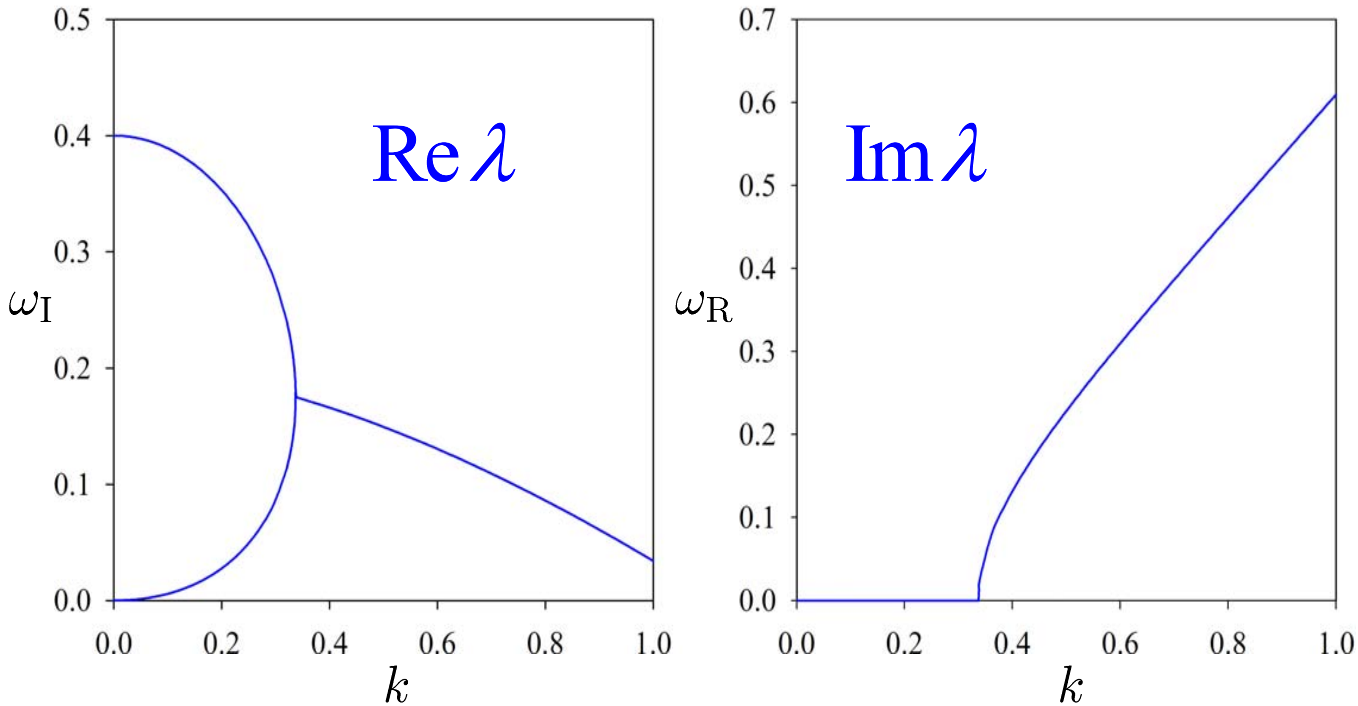

Suspensions of *pushers* are *unstable* at long wavelengths.

pullers are stable

(eigen-solutions do not describe small-scale behavior – Hohenegger & Shelley '09)

Eigenfunctions:

$$\tilde{c}_{\mathbf{k}} = \int dS_p \tilde{\Psi}_{\mathbf{k}}(\mathbf{p}) = 0$$

no concentration fluctuations in linear theory.

$$\tilde{\Sigma}^a_{\mathbf{k}} = \mathbf{k}\mathbf{k}_\perp + \mathbf{k}_\perp\mathbf{k}$$

active stress eigen-modes are shear-stresses.

Non-linear simulations (2-d)

- **Initial condition:** $\Psi(\boldsymbol{x}, \phi, 0) = \frac{1}{2\pi}\left[1 + \sum_i \epsilon_i \cos(\boldsymbol{k}_i \cdot \boldsymbol{x} + \xi_i) \times P_i(\cos\phi, \sin\phi)\right]$

Concentration field *c*

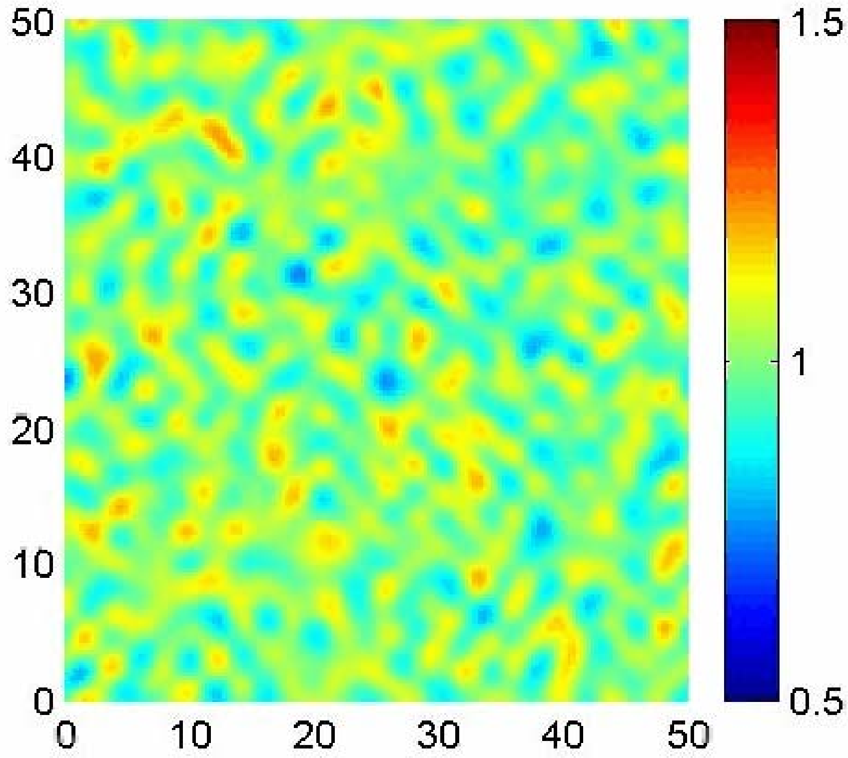

Mean director field ***n***

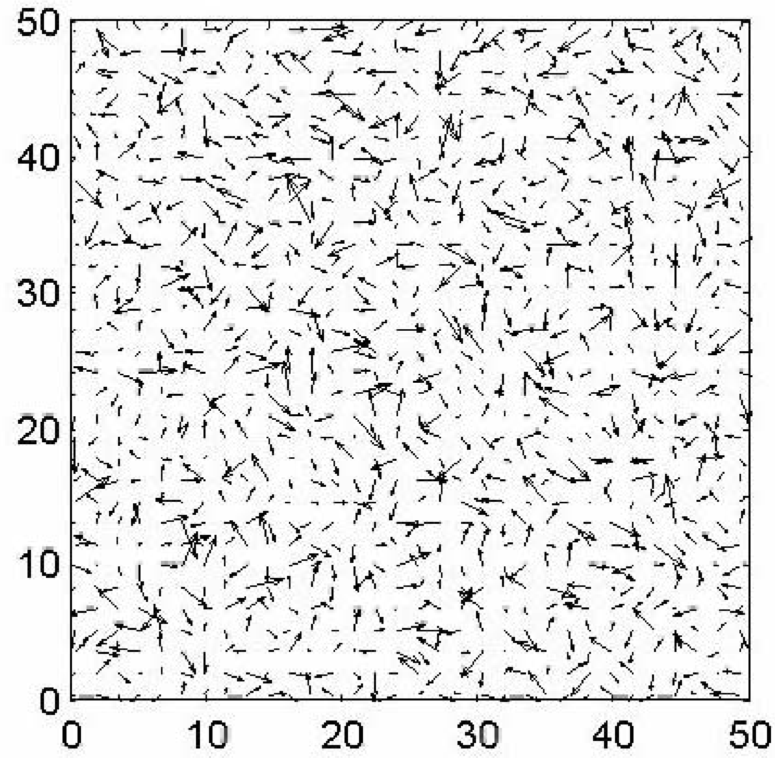

Long-time dynamics: velocity field

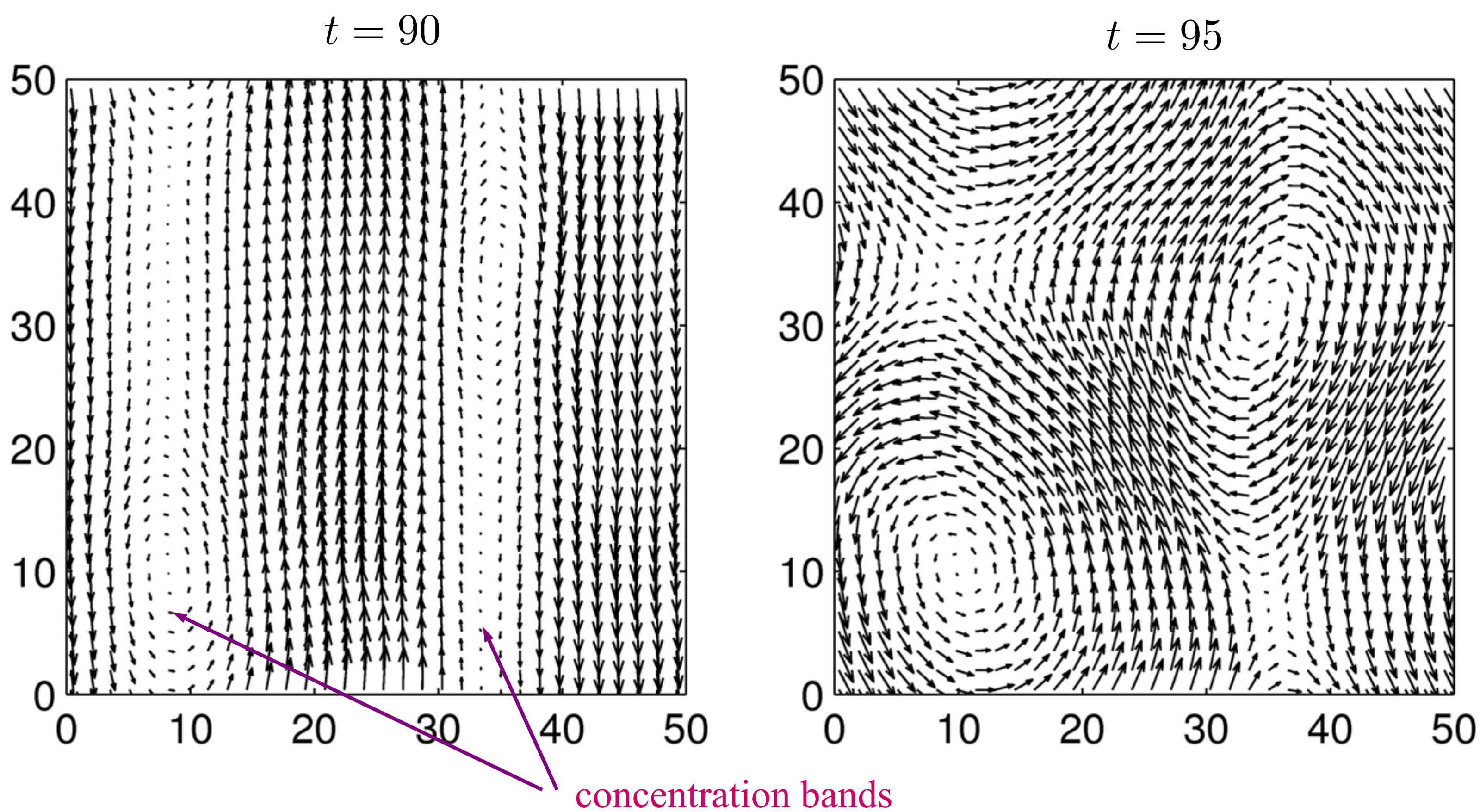

- The concentration bands are located inside shear layers.
- These shear layers become unstable, leading to the formation of vortices and to the break-up of the bands, which then reform in the transverse direction.

Configurational entropy:

$$\begin{cases} S = \int dV_x \int dS_p \left(\frac{\Psi}{\Psi_0}\right) \ln\left(\frac{\Psi}{\Psi_0}\right) \\ \geq 0; \; =0 \text{ only for } \Psi \equiv \Psi_0 \end{cases}$$

$$\Rightarrow \frac{dS}{dt} = \frac{3}{\alpha \Psi_0} \int dV_x \, \mathbf{E} : \mathbf{\Sigma}^a - \frac{1}{\Psi_0} \int dV_x \int dS_p \Psi \left[D \left|\nabla_x \ln \Psi\right|^2 + d \left|\nabla_p \ln \Psi\right|^2 \right]$$

But ... from the momentum equations:

$$P_a(t) = -\int dV_x \, \mathbf{E} : \mathbf{\Sigma}^a = 2 \int dV_x \, \mathbf{E} : \mathbf{E}$$

rate of viscous dissipation balances the active power input $P_a(\mathrm{t})$ of the swimmers

$$\Rightarrow \boxed{\frac{dS}{dt} = \frac{-6}{\alpha \Psi_0} \int dV_x \left|\mathbf{E}\right|^2 - \frac{1}{\Psi_0} \int dV_x \int dS_p \Psi \left[D \left|\nabla_x \ln \Psi\right|^2 + d \left|\nabla_p \ln \Psi\right|^2 \right]}$$

Pullers ($\alpha>0$): fluctuations, as measured by S, will dissipate.

Pushers ($\alpha < 0$): the input power increases fluctuations, until limited by diffusive processes.

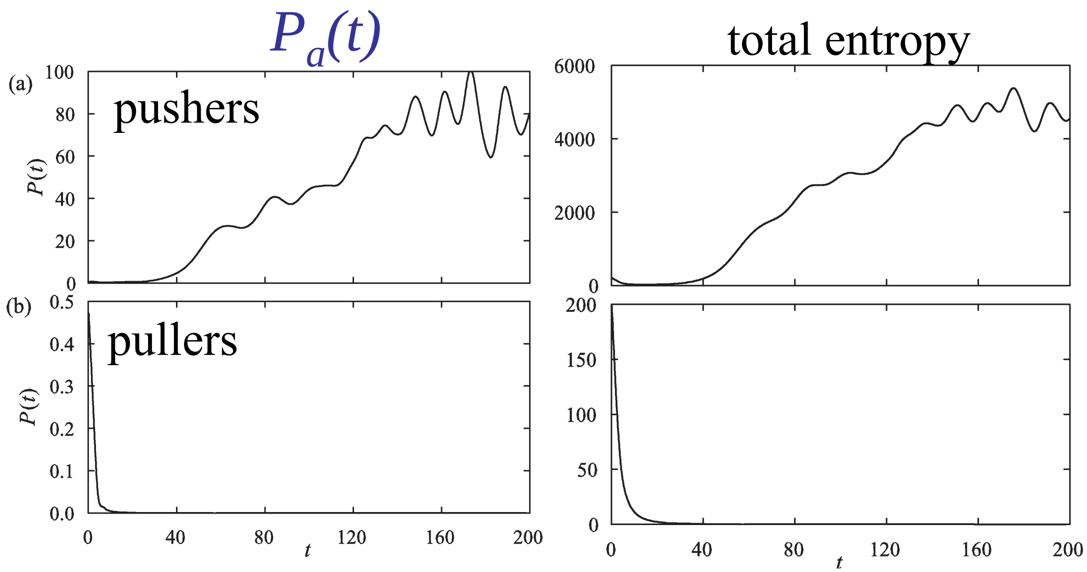

entropy growth saturates; system in statistical equil.

fluctuations in puller suspension quickly dissipate

Active swimmer power density:

$$p(\mathbf{x},t) = -\int dp \left(\alpha \mathbf{p}^{\mathrm{T}} \mathbf{E}(\mathbf{x},t)\mathbf{p}\right)\Psi(\mathbf{x},\mathbf{p},t); \quad P_a(t) = \int dV_x\, p(\mathbf{x},t)$$

For $P_a(t)$ to be positive w. $\alpha<0$, expect $\mathbf{p}$ to be aligned with extensional axis of $\mathbf{E}$

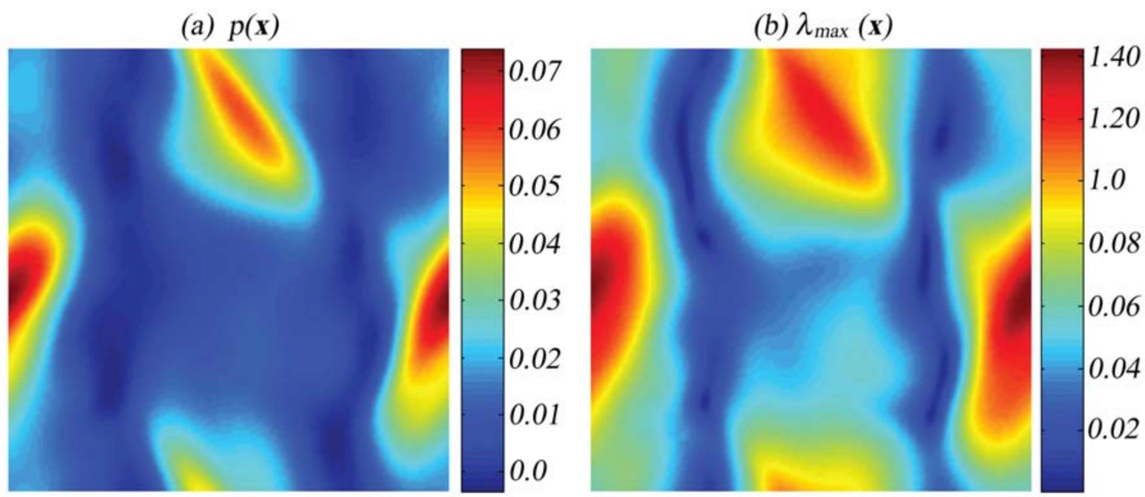

Mixing by active suspensions

Efficient convective fluid mixing is achieved by stretching and folding of fluid elements during the formation and break-up of the concentration bands.

After approximately 4 cycles, good mixing is achieved in the suspension.

From Mathew *et al* '07:

mixing norm": $|| s ||_{H^{-1/2}}$

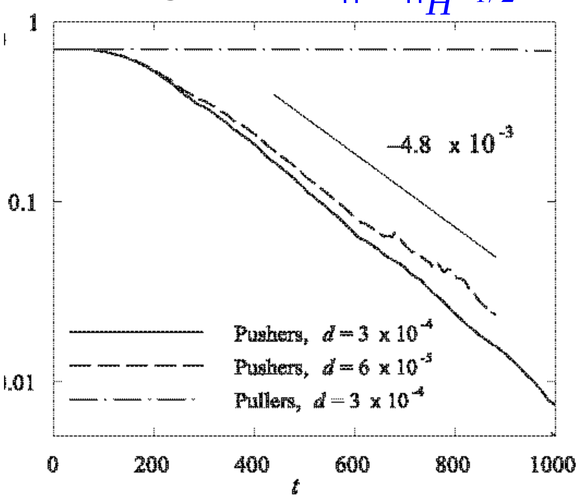

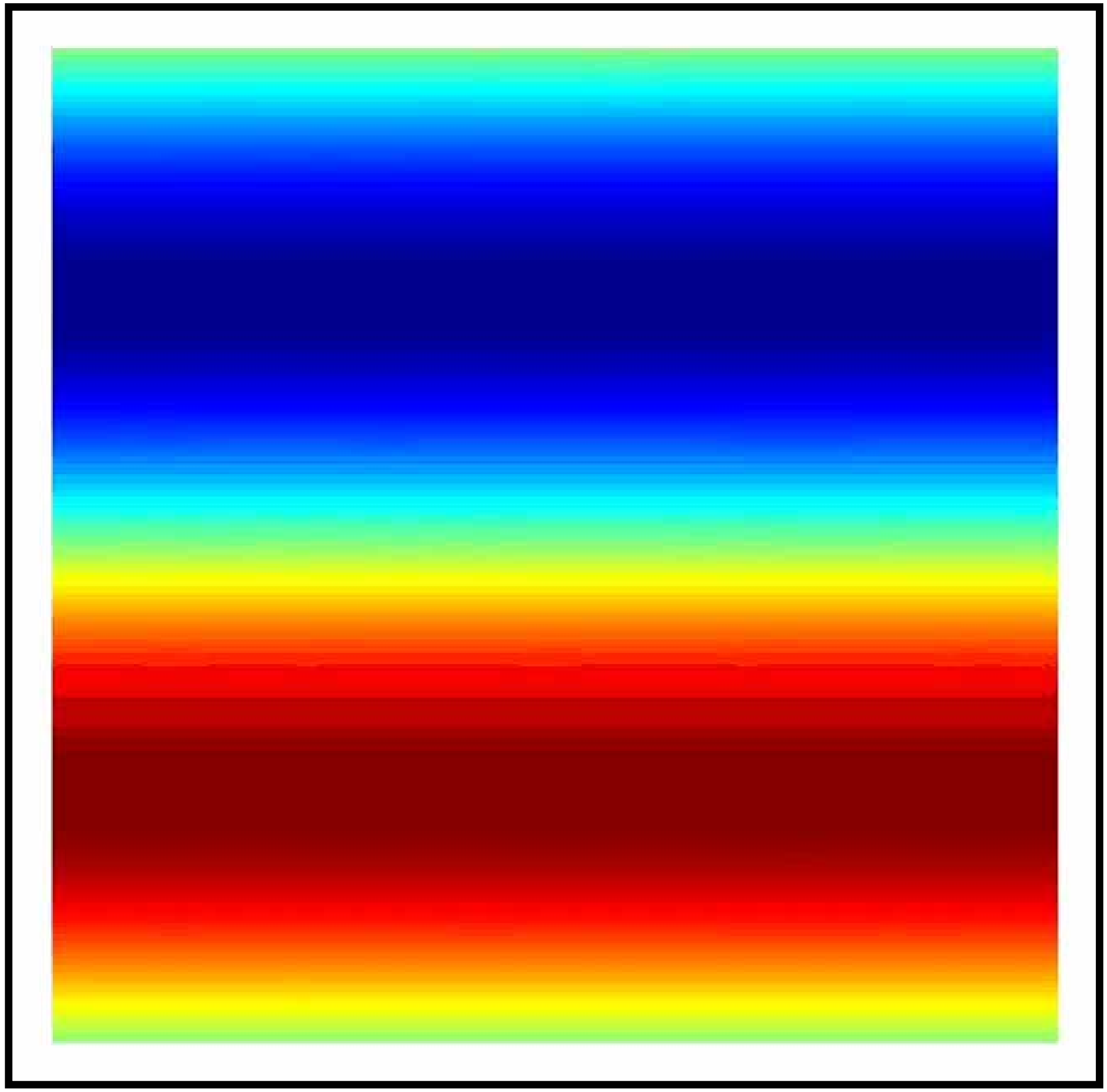

Conclusions

- **Aligned suspensions of swimming rods destabilize as a result of hydrodynamic interactions.**
- **The chaotic flow fields arising in suspensions of swimming rods are dominated locally by near uniaxial extensional (pushers) and compressional (pullers) flows.**
- **At steady state, particle orientations show a clear correlation at short length scales owing to the disturbance flow and to hydrodynamic interactions. This correlation results in an enhancement (or decrease) of the mean particle swimming speed.**
- **Dynamics in thin liquid films are characterized by a strong particle migration towards the gas/liquid interfaces.**

- **Kinetic theory predicts instabilities for both aligned and isotropic suspensions. In the isotropic case, the instability is driven by the particle shear stress.**
- **Non-linear simulations show that active suspensions evolve toward non-uniform distributions as a result of these instabilities. More precisely, the shear stress instability causes the local polar alignment of the particles, which in turn results in the formation of concentration inhomogeneities.**